

Isostaticity and Mechanical Response of Two-Dimensional Granular Piles

Akihiro Kasahara and Hiizu Nakanishi

Department of Physics, Kyushu University 33, Fukuoka 812-8581, Japan

Abstract

We numerically study the static structure and the mechanical response of two-dimensional granular piles. The piles consist of polydisperse disks with and without friction. Special attention is paid for the rigid grain limit by examining the systems with various disk elasticities. It is shown that the static pile structure of frictionless disks becomes isostatic in the rigid limit, while the isostaticity of frictional pile depends on the pile forming procedure, but in the case of the infinite friction is effective, the structure becomes very close to isostatic in the rigid limit. The mechanical response of the piles are studied by infinitesimally displacing one of the disks at the bottom. It is shown that the total amount of the displacement in the pile caused by the perturbation diverges in the case of frictionless pile as it becomes isostatic, while the response remains finite for the frictional pile. In the frictionless isostatic pile, the displacement response in each sample behaves rather complicated way, but its average shows wave like propagation.

PACS numbers: 45.70.-n, 45.70.Cc, 83.80.Fg

I. INTRODUCTION

A pile of granular material is often modeled as an assembly of rigid particles. This simple picture, however, causes some conceptual difficulties when one considers force distribution, or stress, in the pile.

In an ordinary solid that consists of atoms, which are deformable elements, the stress inside is determined by the stress balance equations with the constitutive relation between the stress and strain. No deformation is allowed, however, in rigid elements, in which case the forces acting on each element cannot be determined uniquely for a given configuration in general.

There is a special class of stable pile structures called isostatic, or marginally rigid: A pile structure is isostatic when the forces acting between the elements are uniquely determined only from externally applied forces and the pile structure without any information on deformation of the elements. For such a pile, the total number of balance equations for the forces and torques acting each particle should be equal to the number of independent components of forces, which means the average coordination number z is $2d$ for frictionless spheres and $d + 1$ for frictional spheres or aspherical particles in d -dimensions if the pile is isostatic.

In a real pile the isostaticity is not always satisfied; in the overconstrained case, where the number of conditions is larger than the number of forces, the pile is unstable because there are no sets of force that satisfy the balance equations. On the other hand, in the underconstrained case, where the number of conditions is smaller than the number of forces, the forces cannot be determined uniquely from the macroscopic structure information of the pile; the macroscopic friction force depends on the piling history. It has been conjectured that a stable pile of frictionless rigid particles forms an isostatic structure[1].

The isostaticity of a pile structure has been tested numerically and experimentally for both the frictionless and frictional cases by counting the coordination numbers. Makse *et al.*[2] have performed numerical simulations for three dimensional sphere systems without the gravity and made compact aggregates of balls by compressing the systems by pushing the surrounding walls. By examining the coordination numbers in the zero-pressure limit, they concluded both the frictionless and frictional sphere systems become isostatic in the rigid limit. On the other hand, Silbert *et al.*[3] have also performed numerical simulations on

the three-dimensional sphere system, but the way they made piles is different from that of Makse *et al.* They released the particles in the system at once under the gravity and waited until all the particles stop. Their conclusion is that the frictionless pile becomes isostatic in the rigid limit, but the structure of frictional pile depends on the piling procedure and never becomes isostatic. Blumenfeld and Ball[4, 5] have done simple table top experiments on the pile of two-dimensional non-circular grains made of cardboard. Piles are formed by collecting the grains scattered initially on a horizontal surface by sliding an open rectangular frame. They found that the higher the starting density of grains is, the more cooperative reconfiguration is taken place before they are stuck with each other, and the lower the ending pile density. They have concluded that the isostatic structure of frictional grain is achieved in the limiting case where the starting and ending density coincide.

The isostatic structure, if it is realized in a real pile, should be reflected in the mechanical properties of the rigid granular pile. The mechanical properties of frictionless isostatic structure has been studied in some detail, and it has been shown that (i) the force chain may be regarded as propagating unidirectionally[6], (ii) there is a correspondence between the force-force response and the displacement-displacement response[7], and (iii) the piles are very sensitive to an external perturbation[1]; These features may correspond with some properties of frictionless rigid granular pile.

Regarding the mechanical response of the isostatic pile, using a simple lattice model of isostatic structure, Moukarzel[1] has shown that the total response to an external perturbation diverges as the system approaches to the isostaticity due to the “pantograph effect”. As for the effects of friction, Moukarzel *et al.*[8] have performed experiments on the two-dimensional rigid disk system and demonstrated that the displacement response function has the single peak Gaussian shape with diffusive broadening. They also performed computer simulations on the two-dimensional frictionless disk system and showed that the displacement response function have a double peaked shape with the wave like propagation, suggesting the friction plays an important role in the mechanical response.

In this paper, we present the detailed results of our numerical simulations[9] on the two-dimensional frictionless and frictional disks to show how the isostatic piles are formed for frictionless and frictional disks. We also investigate the mechanical response of the isostatic piles to an external perturbation, and demonstrate there exist important differences in the response between the frictionless and frictional piles when they approach the isostaticity.

After introducing the model and piling procedures in Sec. 2, we present the results for the static pile structure for frictionless and frictional disks in Sec. 3. The mechanical responses are investigated in Sec. 4. The summary of our results is given in Sec. 5.

II. MODEL

We perform molecular dynamics simulations on the system that consists of two-dimensional disks with linear elasticity and damping, which is usually called DEM (Discrete Element Method) in the engineer community. The system is polydisperse with a uniform distribution in the disk diameter over the range between $0.9\sigma_0$ and σ_0 , with σ_0 being the maximum diameter. The masses of the disks are assumed to be proportional to their areas: the mass of the disk with the diameter σ_0 is denoted by m_0 . The bottom of the system is made rough by attaching the disks with the interval σ_0 , and we employ the periodic boundary condition in the horizontal direction. The number of disks N in the system is typically 400, and the horizontal length of the system is $20\sigma_0$, thus we have approximately 20 layers of disks on average.

Piles are formed by letting the system run under gravity with the acceleration g from initial configurations until all the disks stop moving.

The disk at the position $\mathbf{x}(t)$ with mass m follows the Newtonian equation

$$m\ddot{\mathbf{x}}(t) = \mathbf{F}(t), \quad (1)$$

where the force $\mathbf{F}(t)$ consists of the gravitational and contact forces from the neighboring disks in contact. We also use the “viscous equation”

$$\gamma\dot{\mathbf{x}}(t) = \mathbf{F}(t) \quad (2)$$

for some cases to examine the effect of friction because the system that follows eq. (2) is stuck as soon as the force balance is achieved and is more affected by the friction.

The two particles i and j at $\mathbf{x}_i(t)$ and $\mathbf{x}_j(t)$ with radii r_i and r_j , respectively, are in contact when the overlap δ_{ij} given by

$$\delta_{ij} = r_i + r_j - |\mathbf{x}_i - \mathbf{x}_j| \quad (3)$$

is positive. Then the particle j exerts the force \mathbf{F}_{ij} on the particle i

$$\mathbf{F}_{ij} = \mathbf{F}_{ij}^n + \mathbf{F}_{ij}^t, \quad (4)$$

where \mathbf{F}_{ij}^n and \mathbf{F}_{ij}^t are the normal and tangential components of the force:

$$\mathbf{F}_{ij}^n = k_n \delta_{ij} \hat{\mathbf{n}}_{ij} - \gamma_n \mathbf{v}_{ij}^n, \quad (5)$$

$$\mathbf{F}_{ij}^t = -k_t \Delta s_{ij} \hat{\mathbf{t}}_{ij} - \gamma_t \mathbf{v}_{ij}^t. \quad (6)$$

Here, $\hat{\mathbf{n}}_{ij}$ and $\hat{\mathbf{t}}_{ij}$ are the normal and tangential unit vectors, respectively; Δs_{ij} is the tangential displacement of the contact points after the contact, \mathbf{v}_{ij}^n (\mathbf{v}_{ij}^t) is the normal (tangential) relative velocity, k_n (k_t) is the normal (tangential) elastic constant, and γ_n (γ_t) is the normal (tangential) damping constant. Note that we assume no threshold for the disks to slip during the contact in eq.(6), which corresponds to the case with the infinite friction coefficient. In the case of the frictionless disk, we simply set $\mathbf{F}_{ij}^t = \mathbf{0}$.

In the actual simulations, we use $\gamma_n = 2\sqrt{k_n} [\sqrt{m_0}]$ for the frictionless case, and $k_t = 0.2k_n$ and $\gamma_n = \gamma_t = 2\sqrt{k_n} [\sqrt{m_0}]$ for the frictional case. In the simulations with the viscous equation (2), we take $\gamma = 5[m_0\sqrt{g/\sigma_0}]$ with $\gamma_n = \gamma_t = 0$ in eqs.(5) and (6).

III. STATIC STRUCTURE OF PILES

First, we study the isostaticity of granular pile formed through several procedures.

Isostaticity is most easily checked by counting the average number of particles in contact with each particle, namely the average coordination number z . In order that the force acting between particle can be determined only by the contact network structure, the number of independent components of force should be equal to the number of force and torque balance equations. In the case of frictionless spherical grain, the number of independent force components is $zN/2$ because the contact forces have only radial component. The torque of each particle always balances and the number of force balance equation is Nd , therefore, we have $z = 2d$ for the isostatic structure of frictionless spheres in d -dimensions. In the case of frictional grain, we have $z = d + 1$ for both spherical and non-spherical grain, because the number for independent force components is $zdN/2$ and the number of the force and torque balance equations are dN and $d(d - 1)N/2$, respectively.

We perform molecular dynamics simulations to construct piles of frictionless and frictional disks using several procedures. We try two types of initial configurations: the triangular lattice and the random configuration (Fig. 1); the triangular lattice with the lattice constant σ_0 is not a regular lattice because the disks located at the lattice points are polydisperse.

The random configurations are prepared by randomly arranging disks with an area fraction of approximately 0.6.

Simulations to form piles start from these configurations with zero particle velocity and finish when the kinetic energy of each disk becomes negligibly small, namely, smaller than $10^{-15}[m_0 g \sigma_0]$. The number of disks N is 400 and the system size is $20\sigma_0$ in the horizontal direction, thus the number of layers in depth is 20 on average. We also try both eqs. (1) and (2) for the time development.

Figure 2(a) shows the k_n -dependence of the coordination number z for the frictionless disks. It can be seen that the results does not depend on the preparation procedures very much and z converges to a number very close to 4 in the large k_n limit for both initial configurations and time developments. The k_n -dependence is well represented by the power law

$$z - z_\infty \propto k_n^{-\alpha} \quad (7)$$

as is shown in Fig. 3(a). The parameters z_∞ and α are tabulated in Table I.

As for the case of frictional disks, the results are shown in Fig. 2(b). There are two things to be noted in comparison with the frictionless case: (i) the discrepancy among different preparation procedures is larger in the frictional case, and (ii) the limiting values of the coordination number are substantially different from 3, *i.e.* the value for the isostatic structure of the frictional grain in two dimensions (Table I).

There seems to be, however, the tendency that the limiting value of the coordination number z_∞ becomes closer to 3 in the case where the friction may produce more random pile configuration; namely from the Newtonian with the triangular lattice initial configurations to the viscous equation with the random initial configuration.

These results should be compared with those by Silbert *et al.* [3] They also constructed granular piles using DEM and concluded that the piles of frictionless spheres become isostatic in the rigid limit but that of frictional spheres does not become isostatic.

The major difference between the present work and that of Silbert *et al.* lies in the following points: Silbert *et al.* [3] studied the three dimensional systems of mono-disperse spheres with a finite friction constant that follows the Newtonian equation while we investigate the two-dimensional system of polydisperse disks with the infinite friction constant that follows the Newtonian or the viscous equation. Both agree in the point that the pile structure in the frictional systems does not become isostatic in the same way as it does in the frictionless

system, but our results suggest that the isostaticity is achieved even for a frictional system in the certain limiting situation where the friction becomes very effective.

To examine how this discrepancy arises, we plot the distribution of the ratio ζ of the tangential force to the normal force at each contact. The comparison between the pile formed via the Newtonian equation and the pile via the viscous equation from the random initial configurations is given in Fig. 4 for the disk elasticity $k_n = 10^6 [m_0 g / \sigma_0]$, in which case the coordination numbers of the piles are $z = 3.18$ for the Newtonian equation and $z = 3.06$ for the viscous equation. For the both cases we use the random initial configurations. One can see that the pile by the viscous equation contains more contacts with very large value of ζ , while the pile by the Newtonian equation has only contacts with ζ smaller than 10 even though the infinite friction coefficient allows any value of ζ .

If we use a finite value for the friction coefficient, some of the contacts in the pile via the viscous equation would slip to make the pile denser. This would results in a larger average coordination number, which means the pile structure becomes further away from isostatic.

From these observations, we conclude that the infinite friction coefficient and the viscous equation for the time development in the pile forming process from a random initial configuration makes the friction very effective, as a result, the pile becomes so decompacted that it becomes nearly isostatic.

IV. MECHANICAL RESPONSE OF PILES

Now, we study the mechanical response of the frictionless and frictional piles to the external perturbation and see how the response changes as the pile becomes closer to the isostatic. The perturbation is given by displacing one of the disks attached at the floor by $\delta \mathbf{r}_0$ in the upward direction very slowly, and we observe the displacement of each disk $\delta \mathbf{r}_i$ caused in the pile by it.

In order to examine properties of a given contact network, the size of the external displacement is taken small enough that the perturbation does not cause any change in the connectivity of the contact network in the pile. In the simulation, we take the external displacement as $\delta \mathbf{r}_0 = (0, m_0/k_n)$, namely, the order of disk deformation. For such small external displacement, we have checked that the contact network in the pile does not change,

and $\delta \mathbf{r}_i$ is proportional to $\delta \mathbf{r}_0$ thus the relative displacement \mathbf{d}_i defined by

$$\mathbf{d}_i \equiv \frac{\delta \mathbf{r}_i}{|\delta \mathbf{r}_0|} \quad (8)$$

does not depend on $|\delta \mathbf{r}_0|$.

The initial piles are prepared by the way described in the previous section with the random initial configuration and the Newtonian equation. The system size is $60\sigma_0$ in the horizontal direction and the number of disks N is 1200, thus the average number of layers in the depth is 20.

Examples of pile response to the perturbation are shown in Fig.5. The filled disks in the bottom layer are fixed except one at the center marked with a red arrow, which disk is displaced upward. The directions and the distances of the displacements of the disks in the pile are shown by the colored arrows: the red, green and black arrows denotes the displacements $|\delta \mathbf{d}_i| \geq 1$, $0.5 \leq |\delta \mathbf{d}_i| \leq 1$, and $0.1 \leq |\delta \mathbf{d}_i| \leq 0.5$, respectively. The disks that move less than $0.1\delta r_0$ are not marked. One can see the effects of the perturbation extend over long distance in the upper case, namely, the frictionless pile close to the isostaticity, while the effects decay within a short distance in the lower pile of frictional disks.

A. Total Longitudinal Response of Displacement

As a measure of response to the perturbation, we define the total response of displacement in the y -direction D_y , or the total longitudinal response, as

$$D_y \equiv \sum_{i=1}^N \left| \frac{\delta y_i}{\delta y_0} \right| = \sum_{i=1}^N |d_{iy}|, \quad (9)$$

where δy_i is the y component of the displacement for the i -th disk. This quantity should be finite if the response is confined within a finite region, but can diverge in the infinite system if the response extend to the infinity.

The results are shown in Fig.6(a), where the total response D_y is plotted as a function of k_n with which the examined piles are formed by the Newtonian equation from the random initial configuration.

The marks \odot 's (\blacksquare 's) in Fig.6(a) denote the total response D_y of the frictionless (frictional) disks in the frictionless (frictional) piles, respectively.

In addition to these, we examine the frictional response to the perturbation in the frictionless piles (\square 's); namely, the response is calculated using the frictional interaction between disks, although the pile itself is prepared using the frictionless interaction, thus the pile structure has larger coordination numbers than that of real frictional piles with the same elastic constant k_n .

In Fig.6(b), the same data are plotted against the coordination number z of the pile. One can see that the total response of the frictionless pile tends to diverge as z approaches 4, while it remains finite for the frictional pile as $z \rightarrow 3$. It is interesting to see that the frictional responses of the frictionless piles are almost on the same curve with the frictional responses of the frictional piles when they are plotted against z , which suggests that the coordination number characterizes the mechanical response of the pile very well.

B. Spatial Variation of Absolute Value of Longitudinal Response

To understand the diverging total responses in the frictionless isostatic pile, we plot the averaged behavior of the spatial variation of absolute value of longitudinal response $\hat{d}_y(\mathbf{r})$ defined by

$$\hat{d}_y(\mathbf{r}) \equiv \langle \sum_{i=1}^N |d_{iy}| \delta(\mathbf{r} - \mathbf{r}_i) \rangle, \quad (10)$$

where $\langle \dots \rangle$ denotes the statistical average. This quantity is related to D_y by

$$D_y = \int \int d\mathbf{r} \hat{d}_y(\mathbf{r}). \quad (11)$$

In actual calculations, the spatial variation is calculated on a grid with the mesh spacing σ_0 and the average is taken over a few hundreds realizations.

The results are shown in Fig.7, where $\hat{d}_y(\mathbf{r})$'s are plotted against x and y with the contour lines; The perturbation is applied at $(x, y) = (0, 0)$.

We examine the two cases, namely, $k_n = 10^3$ and 10^6 [m_0g/σ_0], for both the frictionless and frictional piles; the coordination number $z = 4.86$ and 3.98 for $k_n = 10^3$ and 10^6 [m_0g/σ_0], respectively, for the frictionless pile, and $z = 3.75$ and 3.12 for the frictional pile; The piles with $k_n = 10^6$ [m_0g/σ_0] are closer to the isostatic than those with $k_n = 10^3$ [m_0g/σ_0] for both the frictionless and frictional piles.

Let us examine the frictionless case first. The response in the pile with $k_n = 10^3$ [m_0g/σ_0], which is away from the isostatic, decays quickly as it departs from the point of perturbation.

On the other hand, the situation is quite different for the pile with $k_n = 10^6 [m_0 g / \sigma_0]$, which is close to the isostatic: the response does not decay along the y -axis with $x = 0$, and if one looks along the line parallel to the x -axis with constant y , one sees a plateau region where the response is constant. This plateau region, which seems to extend to the infinity, is responsible to the diverging behavior of the total response D_y .

On the other hand, in the case of frictional pile with $k_n = 10^6 [m_0 g / \sigma_0]$, there is no tendency to develop the plateau region, although the response is larger than that for the pile of $k_n = 10^3 [m_0 g / \sigma_0]$.

C. Averaged Displacement-Displacement Response Function

Finally, we present the displacement-displacement response function $\Delta(\mathbf{r})$ for this external perturbation:

$$\Delta(\mathbf{r}) = \langle \sum_{i=1}^N \mathbf{d}_i \delta(\mathbf{r} - \mathbf{r}_i) \rangle. \quad (12)$$

The average is taken over a few hundreds realizations and the spatial dependence is calculated on a grid with the mesh size σ_0 .

The displacement-displacement response function has been shown to be equal to the force-force response function for a frictionless isostatic structure[7], but it should be noted that this correspondence does not hold in other cases.

The results are shown in Figs. 8 and 9 for the frictionless and frictional piles, respectively, for $k_n = 10^3$ and $10^6 [m_0 g / \sigma_0]$.

$\Delta_x(\mathbf{r})$ is positive for $x > 0$ and negative for $x < 0$ while $\Delta_y(\mathbf{r})$ is always positive when it is averaged.

For both the frictionless and frictional piles, the region where $\Delta(\mathbf{r}) \neq \mathbf{0}$ is larger for the pile whose coordination number z is smaller, namely, for the pile that is closer to the isostatic.

It should be noted that the way $\Delta_y(\mathbf{r})$ extends is very different from that of $\hat{d}_y(\mathbf{r})$, especially in the frictionless pile close to the isostatic. The response function $\Delta_y(\mathbf{r})$ propagates in the y -direction with the double peaked structure when one see it along the line parallel to the x -axis with constant y , while $\hat{d}_y(\mathbf{r})$ develops the plateau region.

This comparison shows that the response to the perturbation is not actually small in the

“low response region” of $\Delta_y(\mathbf{r})$ between the two peaks for the frictionless isostatic pile, but the large response varies from sample to sample and they are averaged out to make $\Delta_y(\mathbf{r})$ small.

The way how this double peaked structure in $\Delta_y(\mathbf{r})$ develops as the frictionless pile approaches to isostatic can be seen in the contour line plots in Fig.10 (a).

The response $\Delta(\mathbf{r})$ in the frictional pile shows smoother structure than that in the frictionless pile and does not seem to develop the double peaked structure as the pile becomes isostatic (Fig.10 (b)).

V. SUMMARY

We have investigated the structure and the mechanical response of the two-dimensional piles of disks with various disk elasticities; The piles are formed through a several deposition procedures under the gravity.

As for the structure, we have shown the followings: The piles of frictionless disks become isostatic when the disks are very hard and they are not very sensitive to the preparation procedure, which is consistent with the conjecture that the pile of rigid grains is isostatic. On the other hand, for the piles of frictional disks with the infinite friction, the structure depends on the preparation process. If the pile is formed from a triangular lattice with the inertia following the Newtonian equation, the pile structure seems to be distinctively different from the isostatic one even in the rigid limit, as has been found in the previous work on the three-dimensional system[3]. We have found, however, that the pile of frictional disks becomes very close to the isostatic one in the rigid grain limit when we employ the deposition process where the infinite friction is effective, namely, the viscous equation is used for the time development for the disks with the infinite friction constant from the random initial configurations.

The role of friction for the frictional isostaticity is demonstrated by examining the distribution of the ratio of the normal force to the tangential force; In the pile that is close to the isostaticity with frictional disks, the distribution of ζ extends to very large value as of order 10^3 . This suggests that the frictional isostaticity is realized only in the cases where the exceptionally large friction coefficient is effective, and most of real stable piles with modest friction should be hyperstatic with history dependent forces even in the rigid limit.

We have also investigated the mechanical response of the piles of frictionless and frictional disks with a special attention on the isostaticity of the pile structure. We have examined the disk displacement caused by moving one of the disks at the bottom of the pile by an infinitesimally small distance. It has been shown that, for the frictionless pile with the isostatic structure, the response does not decay as it departs from the point of perturbation, and the total sum of the disk displacement diverges as the pile becomes isostatic, while the response decays quickly in the pile with structure far from isostaticity. It is found that the averaged longitudinal response Δ_y becomes double peaked in the isostatic frictionless pile.

As for the frictional pile, the response function always decays in a finite distance and the longitudinal response remains single peaked, which behavior does not change drastically as the structure approaches isostatic.

The double peaked structure in the displacement-displacement response function for the frictionless isostatic pile may be compared with the hyperbolic stress propagation in the granular system[10, 11] due to the equivalence between the stress-stress response function and the displacement-displacement response function in the frictionless isostatic pile[7]. The single peaked structure, on the other hand, may correspond to the diffusive stress propagation, but this correspondence is indirect because there is no equivalence between the displacement response and the stress response in the frictional or non-isostatic pile.

It is interesting to note that, in the isostatic piles, the spatial distribution of averaged response of disk displacement Δ_y is clearly different from that of absolute value of disk displacement; the former develops the double peaked structure while the latter shows the plateau structure, namely, in the region between the two peaks where the average displacement is small, the actual displacement response is not small in each sample, but just they are random and averaged out. This means that the averaged displacement response in the isostatic pile appears to propagate like a wave following a hyperbolic equation, but the way that displacement response propagates in each sample is quite complicated and does not look like a wave(Fig. 5).

Acknowledgments

This work is partially supported by Grant-in-Aid for Scientific Research (C) (No. 16540344) from JSPS, Japan.

- [1] C.F. Moukarzel, Phys. Rev. Lett. **81**, 1634 (1998).
- [2] H.A. Makse, D.L. Johnson, and L.M. Schwartz, Phys. Rev. Lett. **84**, 4160 (2000).
- [3] L.E. Silbert, D.Ertas, G.S. Grest, T.C. Halsey and D. Levine, Phys. Rev. E **65**, 031304 (2002).
- [4] R.C. Ball and R. Blumenfeld, Phys. Rev. Lett. **88**, 115505 (2002).
- [5] R.C. Ball and R. Blumenfeld, Phil. Trans. R. Soc. Lond. A **361**, 731 (2003).
- [6] A.V. Tkachenko and T.A. Witten, Phys. Rev. E **60**, 687 (1999).
- [7] C.F. Moukarzel, Granular Matter **3**, 41 (2001).
- [8] C.F. Moukarzel, H. Pacheco-Martínez, J.C. Ruiz-Suarez, arXiv:cond-mat/0308240.
- [9] A. Kasahara and H. Nakanishi, J. Phys. Soc. Jpn. **73**, 789 (2004).
- [10] J. Bouchaud, M. Cates, and P. Claudin, J. de Physique I, **5**, 639 (1995).
- [11] J. Wittmer, M. Cates, and P. Claudin, J. de Physique I, **7**, 39 (1997).

Eq. of motion	Initial config.	Frictionless		Frictional	
		z_∞	α	z_∞	α
Newtonian	Triangular lattice	3.97	0.68	3.15	0.49
	Random config.	3.98	0.65	3.09	0.47
Viscous	Triangular lattice	3.97	0.63	3.06	0.60
	Random config.	3.97	0.64	3.04	0.46

TABLE I: The limiting coordination numbers z_∞ and the exponents α for various preparation procedures.

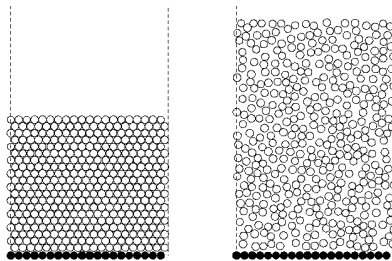


FIG. 1: Two initial configurations: the triangular lattice with polydisperse disks (left) and the random configuration with a number density 0.6 (right).

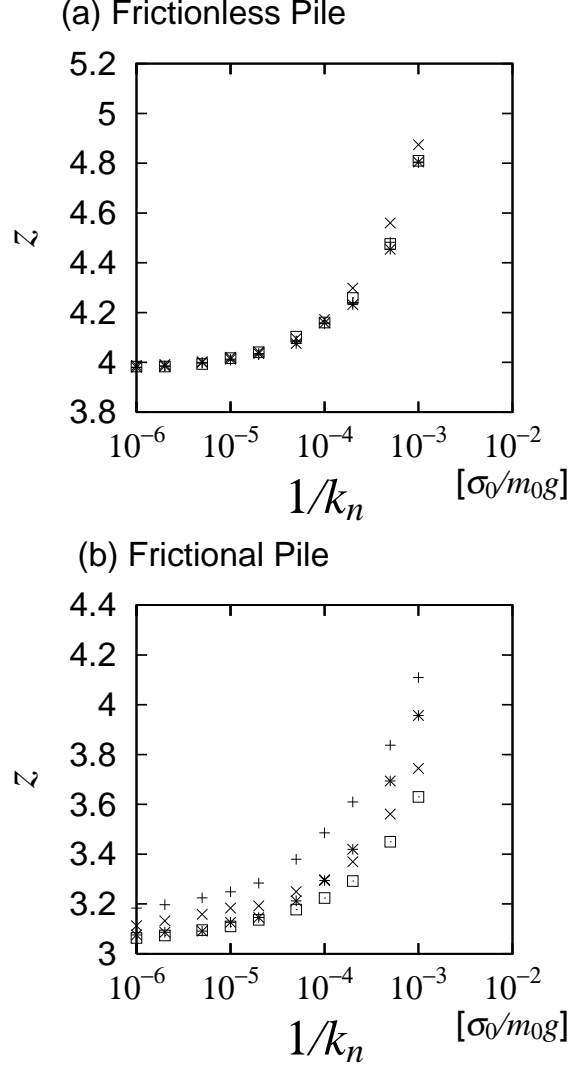


FIG. 2: The coordination number z for various elastic constants k_n for a frictionless pile (a) and frictional pile (b). The marks represent the pile preparation procedure: the Newtonian equation with the triangular lattice initial configuration (+), the Newtonian equation with the random initial configuration (\times), the viscous equation with the triangular lattice initial configuration (*), and the viscous equation with the random initial configuration (\square). Each mark represents the average of six to twelve realizations.

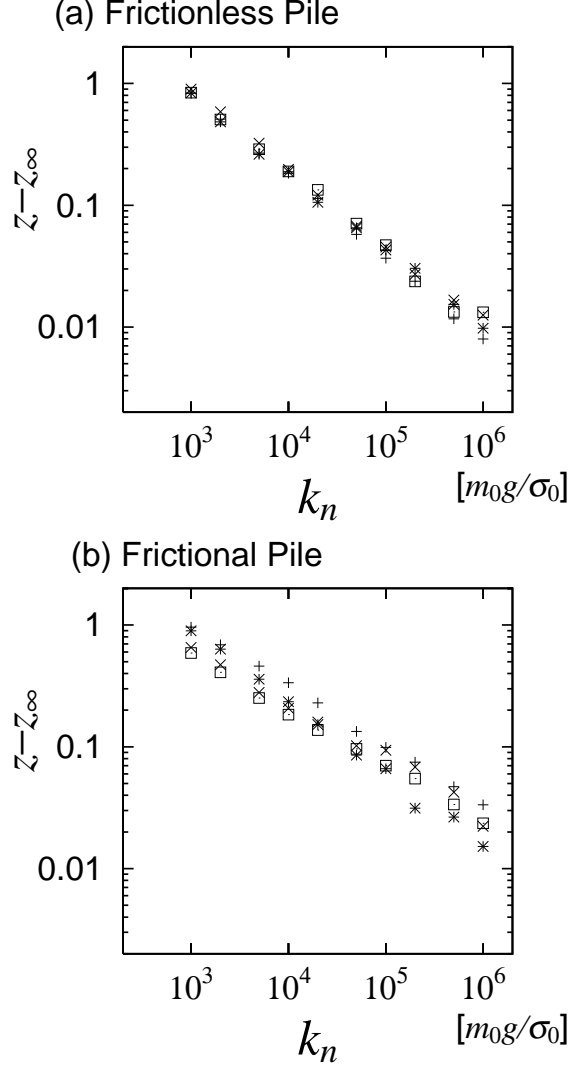


FIG. 3: The coordination numbers $z - z_\infty$ for various elastic constants k_n in the log-log scale for the frictionless pile (a) and the frictional pile (b). The same data are plotted using the same marks as those in Fig. 2 with z_∞ listed in Table I.

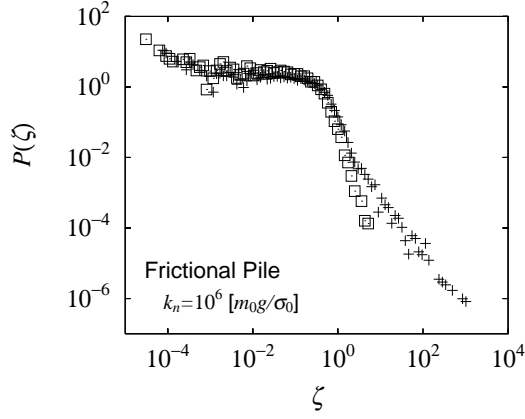


FIG. 4: The distribution for the ratio ζ of the tangential force to the normal force in the piles produced by the viscous equation ($+$) and that by Newtonian equation (\square) from the random initial configurations with the disk elasticity $k_n = 10^6 [m_0 g / \sigma_0]$. The average coordination numbers are $z = 3.06$ for the pile by the viscous equation and $z = 3.18$ for that by the Newtonian equation. Each plot represents average over about ten realizations.

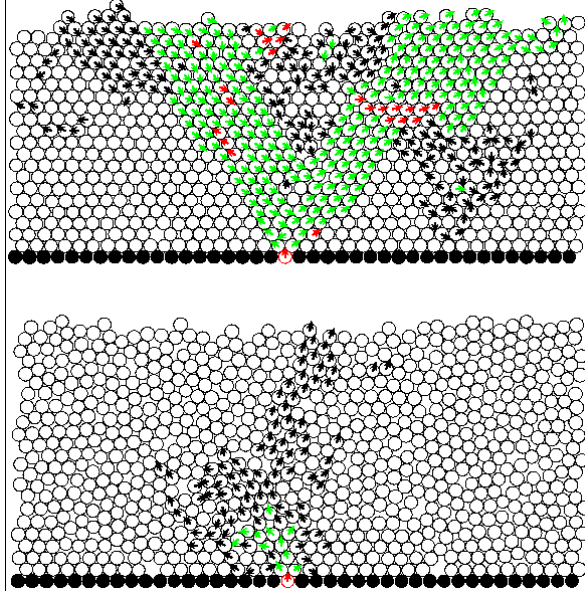


FIG. 5: (Color online) The mechanical response caused by the small displacement of a disk at the bottom (denoted by an open (red) circle with a dark grey (red) arrow) in the frictionless pile (upper) and in the frictional pile (lower) with $k_n = 10^6[m_0g/\sigma_0]$. The dark grey (red), light grey (green), and black allows denote the displacement direction of the disks that move by the distance $\delta r_i \geq \delta r_0$, $0.5\delta r_0 \leq \delta r_i < \delta r_0$, and $0.1\delta r_0 \leq \delta r_i < 0.5\delta r_0$, respectively.

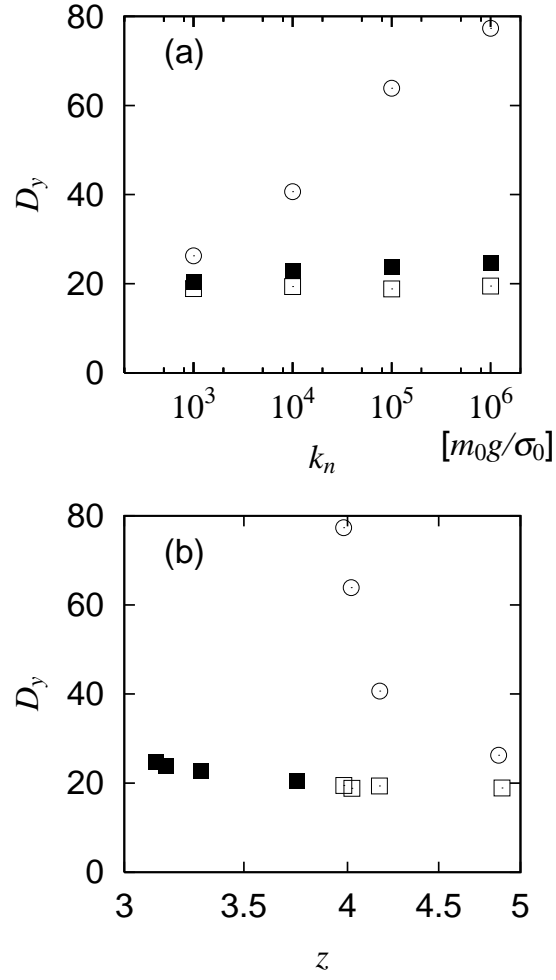


FIG. 6: The total longitudinal displacement D_y caused by the perturbation in the frictionless pile (\odot), in the frictional pile (\blacksquare), and for the frictional response in the piles formed through frictionless dynamics (\square , see text). (a) D_y v.s. the elastic constant k_n . (b) the same data D_y are plotted v.s. the average coordination number of the pile z . Each plot represents average over around 350 realizations.

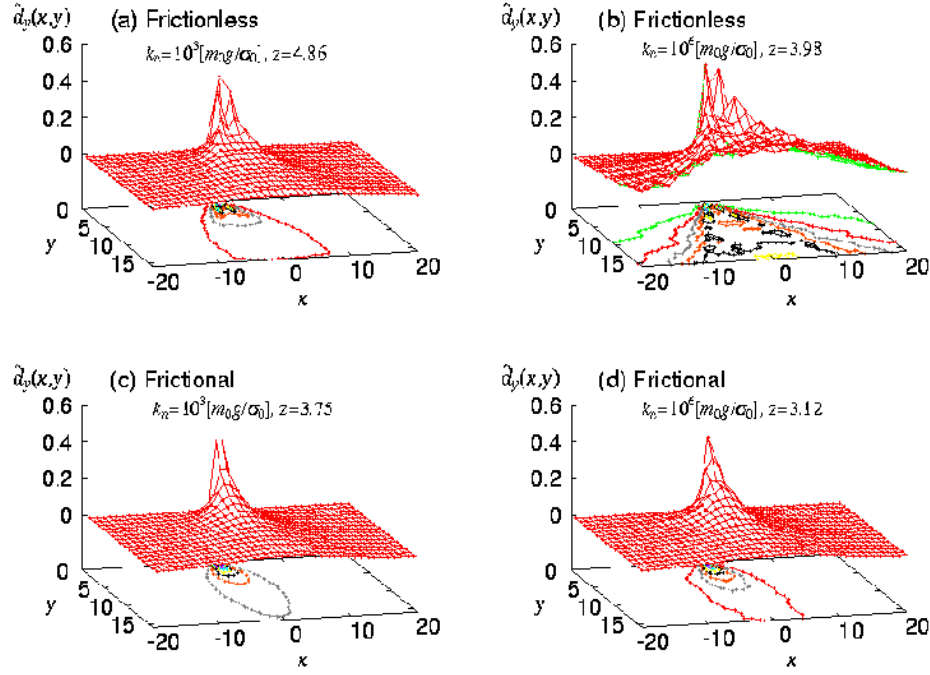


FIG. 7: (Color online) The spatial distribution of the averaged absolute value of the longitudinal response in the frictionless piles (a, b), and in the frictional piles (c, d) with $k_n = 10^3 [m_0 g / \sigma_0]$ and $10^6 [m_0 g / \sigma_0]$. The plots are averaged over a few hundreds realizations.

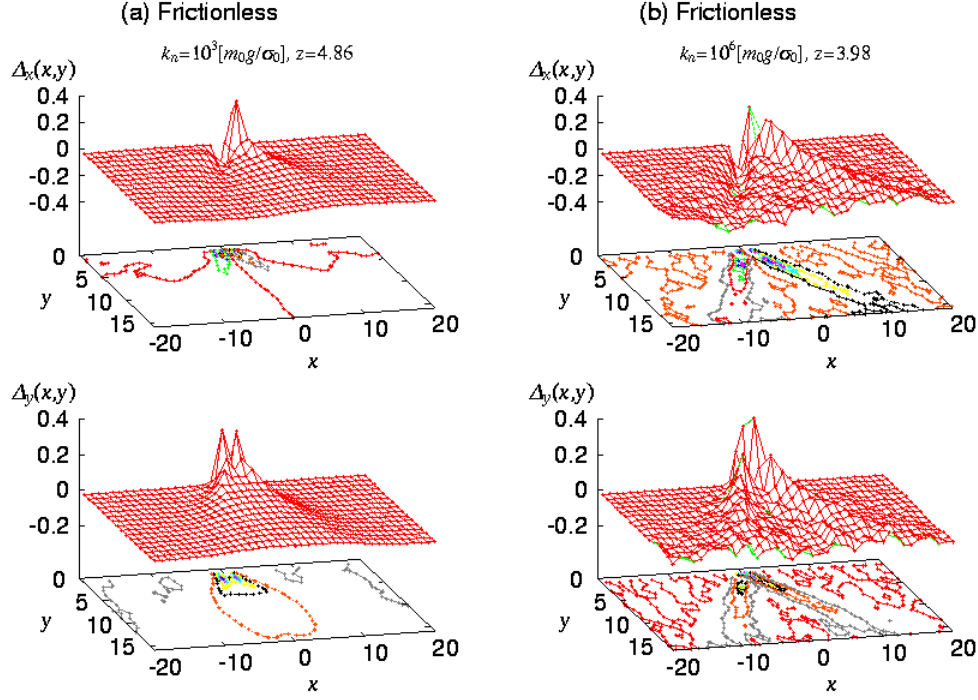


FIG. 8: (Color online) The spatial distribution of the averaged displacement-displacement response function in the frictionless piles with $k_n = 10^3[m_0g/\sigma_0]$ (a) and $10^6[m_0g/\sigma_0]$ (b). The plots are averaged over a few hundreds realizations.

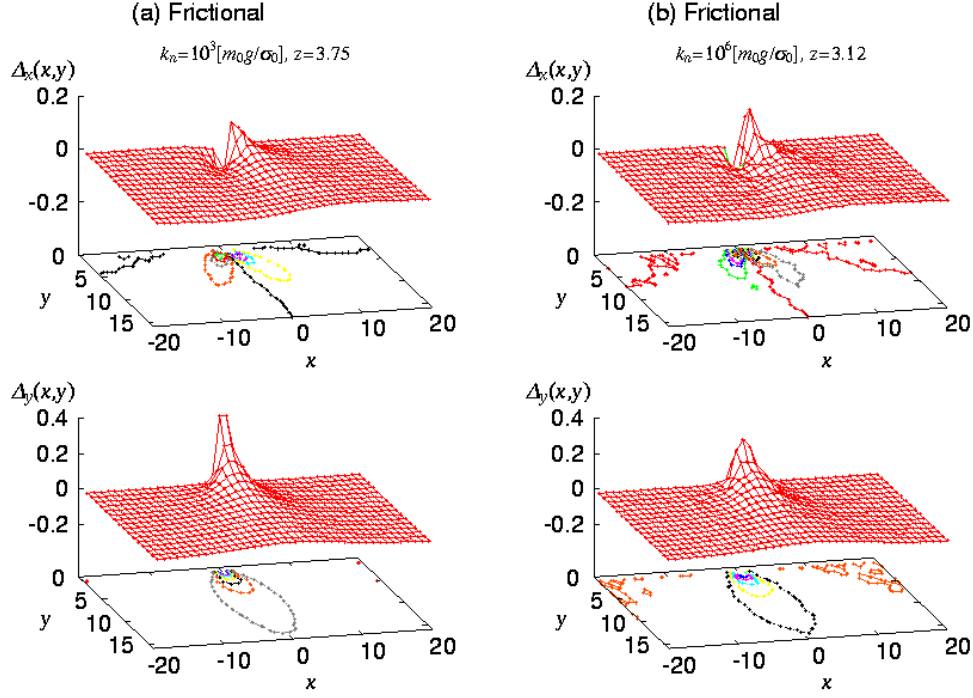


FIG. 9: (Color online) The spatial distribution of the averaged displacement-displacement response function in the frictional piles with $k_n = 10^3 [m_0 g / \sigma_0]$ (a) and $10^6 [m_0 g / \sigma_0]$ (b). The plots are averaged over a few hundreds realizations.

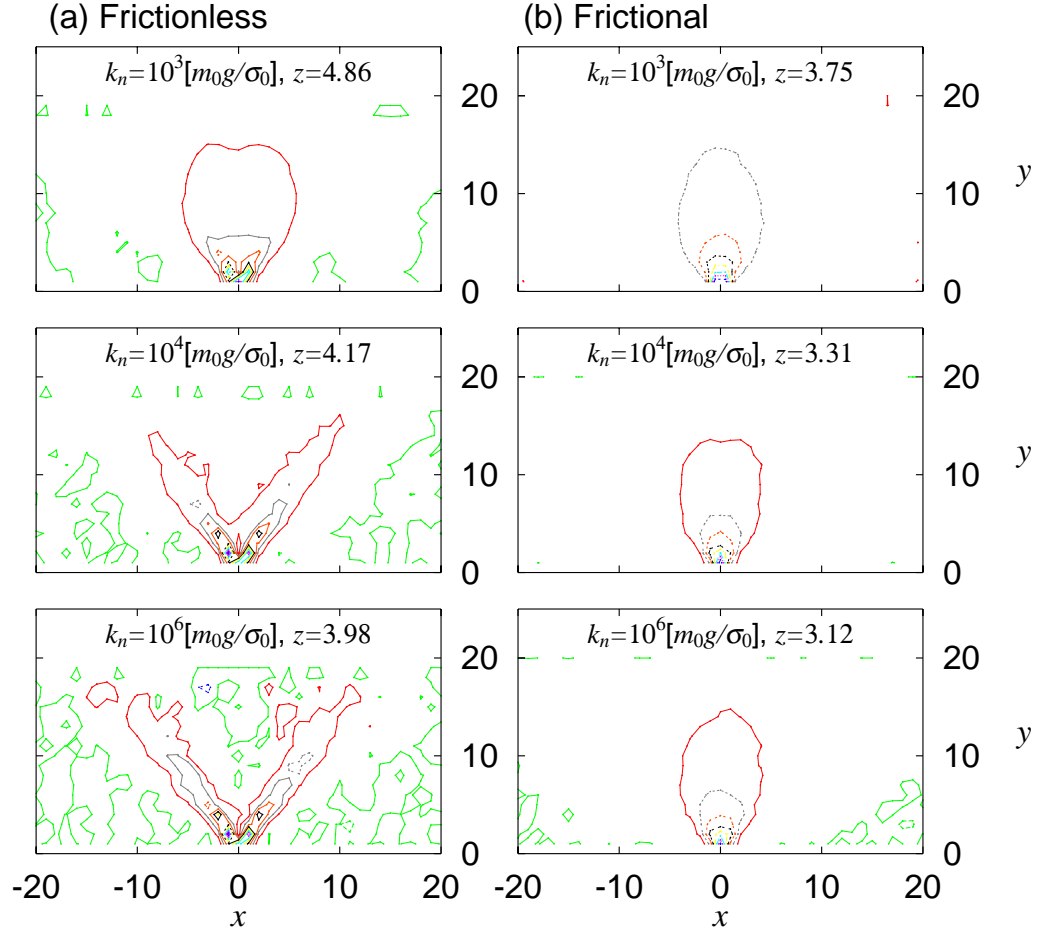


FIG. 10: (Color online) The contour plots of the longitudinal component of displacement-displacement response function Δ_y in the frictionless piles (a) and in the frictional piles (b) with the disk elasticity $k_n = 10^3, 10^4$, and 10^6 $[m_0 g / \sigma_0]$.